RF-signal Transfer Methods for Receive Coils in Integrated Magnetic Resonance Imaging System and Linear Accelerator

Jehki Pusa

School of Electrical Engineering

Thesis submitted for examination for the degree of Master of Science in Technology.

Espoo 9.9.2016

Thesis supervisor:

Prof. Antti Räisänen

Thesis advisor:

M.Sc. Teemu Niemi

Aalto University
School of Electrical
Engineering

AALTO UNIVERSITY
SCHOOL OF ELECTRICAL ENGINEERING

ABSTRACT OF THE
MASTER'S THESIS

Author: Jehki Pusa

Title: RF-signal Transfer Methods for Receive Coils in Integrated Magnetic Resonance Imaging System and Linear Accelerator

Date: 9.9.2016 Language: English Number of pages: 7+29

Department of Radio Science and Technology

Professorship: Radio Science and Engineering

Supervisor: Prof. Antti Räisänen

Advisor: M.Sc. Teemu Niemi

MR-Linac is an integration of an magnetic resonance imaging system and a linear accelerator. It is used to deliver image-guided radiation therapy treatments for patients with cancer. It can deliver higher doses with better accuracy than traditional radiation therapy treatment tools.
The goal of this thesis work was to develop a way to transmit a 63.87 MHz RF-signal through a radiation window in an MR-Linac receive coil. Transmitting the received signal through the radiation window would enable the development of MR-Linac receive coils with higher signal-to-noise ratio and reduced imaging time.
When transmitting signals in the radiation window the transmission lines must be designed to have a minimal linear accelerator radiation attenuation and a sufficient radiation resistance. Three different transmission line methods where tested and compared: micro-coaxial cable, microstrip line and coplanar waveguide.
The most promising results were achieved with the microstrip line. The coplanar waveguide was not usable for the application because of its strong coupling to the surrounding environment.

Keywords: MR-Linac, MRI, receive coil, transmission line

AALTO-YLIOPISTO
SÄHKÖTEKNIIKAN KORKEAKOULU

DIPLOMITYÖN
TIIVISTELMÄ

Tekijä: Jehki Pusa

Työn nimi: RF-signaalin siirtomenetelmiä vastaanottokeloille magneettikuvauslaitteen ja lineaarikiihdyttimen integraatiossa

Päivämäärä: 9.9.2016 Kieli: Englanti Sivumäärä: 7+29

Radiotieteen ja -tekniikan laitos

Professuuri: Radiotekniikka

Työn valvoja: Prof. Antti Räisänen

Työn ohjaaja: DI Teemu Niemi

MR-Linac on magneettikuvauslaitteen ja lineaarikiihdyttimen yhdistelmä. Siinä käytetään magneettikuvia apuna syöpäpotilaiden säteilyhoidossa. Magneettikuvien ansiosta potilaille voidaan antaa paremmalla tarkkuudella suurempia säteilyannoksia kuin perinteisissä säteilyhoitomenetelmissä.

Tämän diplomityön aiheena oli 63,87 MHz:n signaalin siirtäminen MR-Linacin vastaanottokelan säteilyikkunan läpi. Vastaanotetun signaalin siirtäminen säteilyikkunan läpi mahdollistaisi vastaanottokelojen suunnittelun, joilla saavutettaisiin suurempi signaali-kohinasuhde ja lyhyempi kuvausaika.

Siirrettäessä signaalia säteilyikkunassa siirtolinjojen tulee vaimentaa lineaarikiihdyttimen säteilyä mahdollisimman vähän ja kestää korkeaenergisen säteilyn pitkäaikaiset vaikutukset. Kolmea erityyppistä siirtolinjaa testattiin ja vertailtiin: mikro-koaksiaalikaapelia, mikroliuskajohtoa ja koplanaarista johtoa.

Mikroliuskajohdolla saatiin kaikista lupaavimpia tuloksia. Koplanaarinen johto osoittautui tässä käyttötarkoituksessa täysin käyttökelvottomaksi sen voimakkaan kytkennän takia.

Avainsanat: MR-Linac, magneettikuvaus, vastaanottokela, siirtolinja

Preface

Majority of the work done to complete this thesis has been educational, meaningful and at its best intellectually rewarding. However, there were also times when the amount of work has felt crushing and it has been hard to see the light at the end of the tunnel. Especially at such moments of despair I've received support and encouragement from people whom I would like to thank here.

First I would like to thank my advisor and colleague Teemu Niemi for being my guide to the challenging yet fascinating life of electromagnetism and magnetic resonance imaging. Secondly great thanks to my supervisor Antti Räisänen for conducting this thesis to its scientific style and for mentoring the writing process. The vast experience of both of you was enormous help while doing the work and I hope you are as satisfied by the end result as I am.

Next I want to thank my family even though I seriously doubt that any of you will ever take a look inside these covers. You have always been there for me and raised me well which I will always be grateful to you.

Also many thanks to all my colleagues at Philips and especially to Joel Tulppo and Raduma Wycliffe. It has been a pleasure to get to be a part of such a professional and enjoyable working atmosphere.

Lastly a huge thanks belongs to my dearest friends Antti R., Antti V., Juuso, Kalle, Lauri, Miikka, Mikko and Ville. While doing this thesis work you have reminded me that there is more to life than transmission lines or receive coils. Without you my university years would not have been as entertaining as they have been.

Otaniemi, 9.9.2016

Jehki Pusa

Contents

Symbols and abbreviations

Symbols

B_0	Static magnetic field
f_0	Larmour frequency
t	Thickness
Z_0	Characteristic impedance
α	Attenuation
γ	Gyromagnetic ratio
ε	Permittivity
ε_l	Effective dielectric constant
ε_r	Relative permittivity
μ	Permeability
μ/ρ	Mass absorption coefficient [cm^2/g]
ρ	Density
σ	Electrical conductivity

Abbreviations

CPW	Coplanar waveguide
Gy	Gray, measure of absorbed radiation dose [Gy = J/kg]
Linac	Linear accelerator
MCX	Micro-coaxial
MR	Magnetic resonance
MRI	Magnetic resonance imaging
MR-Linac	Integration of an MRI system and a linear accelerator
NMR	Nuclear magnetic resonance
PCB	Printed circuit board
PFA	Perfluoroalkoxy
PI	Polyimide
RF	Radio frequency
Rx	Receive
SENSE	Sensitivity encoding
SNR	Signal-to-noise ratio

1 Introduction

Radiation therapy or radiotherapy is a type of cancer treatment where the purpose is to kill malignant cells with ionizing, high-energy radiation while causing minimal harm to surrounding, healthy organs. The total dose required to kill a tumor (typically from 20 to 80 Gy) is divided over multiple treatment sessions where typically a dose of 2 Gy is delivered. This way the healthy cells have some time to recover from the radiation before the next treatment session.

Exposure to the radiation of the healthy cells surrounding the tumor can be limited by radiating the tumor from different angles and by modifying the beam shape. To be able to use these technques, accurate knowledge of the tumor shape and position is required.

Magnetic resonance imaging (MRI) is a medical imaging technique that enables to image the anatomy of a human body. It has superior soft-tissue contrast compared to other medical imaging techniques such as computed tomography imaging.

MRI-guided radiotherapy means the use of MRI images to improve the radiation treatment deliveries. The possibility to use MRI images as a guidance in dose delivery planning increases the accuracy of the therapy and potentially improves the treatment outcome [1]. While the number of diagnosed cancers keeps increasing, there is a growing need for more efficient radiation treatments. Increased accuracy of MRI-guided therapy compared to traditional radiation therapy enables the use of higher radiation doses which decreases the needed treatment session times.

MR-Linac is an integration of an MRI system and a linear accelerator (Linac) used to generate the high energy radiation. It is used to deliver accurate radiation therapy treatments for patients with cancer. Figure 1 visualizes the structure of an MR-Linac system.

To be Linac compatible the designed MRI system parts must be able to withstand the effects of the Linac radiation and at the same time should cause as little attenuation as possible for the Linac radiation in the so called radiation window. The radiation window is the area that the Linac radiation beam passes through.

The goal of this thesis work was to develop a way to transmit a 63.87 MHz RF-signal through the radiation window in the MR-Linac receive coil. The possibility to transmit the signal through the radiation window would enable the development of MR-Linac receive coils with smaller loop elements which yields to a higher signal-to-noise ratio [2]. It would also enable a loop geometry that would permit the use of sensitivity encoding (SENSE) in head-feet direction. SENSE is an MRI method used to reduce the imaging time [3].

Three different transmission line techniques where chosen to be tested and compared: micro-coaxial cable, microstrip line and coplanar waveguide. The micro-coaxial cable used in the measurements was Temp-Flex 50MCX-37 with PFA as an insulating material and a total diameter of 0.3 mm. The used microstrip lines and coplanar waveguides were designed on 101.6 μm thick DuPont polyimide substrate (DuPont Pyralux AP8545R).

A comparison of the transmission line techniques was done based on their radiation resistance, radiation attenuation and signal-to-noise ratio. Radiation resistance

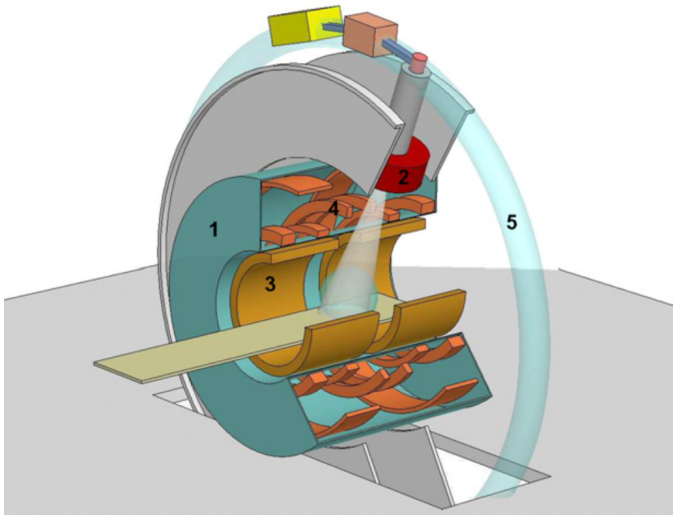

Figure 1: Schematic of the MR-Linac configuration [1]. The linear accelerator (2) is located in a ring around the MRI system (1). The Linac can be rotated over the ring (5) and the radiation can be applied from different angles to the patient. All MRI components in MR-Linac, such as the gradient coils (3) and the superconducting coils (4), have a radiation window where the Linac radiation can travel with a minimal attenuation.

estimation of the transmission lines was done was done based on the literature. Attenuation of the linear accelerator radiation was estimated by theoretical calculations. Signal-to-noise ratio was measured from MR images using each transmission line to transmit the received signal through the radiation window in MR-Linac receive coil.

Chapter 2 gives a background for magnetic resonance imaging, linear accelerator and their integration. The transmission line types used in this thesis work are described in Chapter 3. Chapter 4 presents the design, the measurements and the results of the transmission lines. Calculations for the Linac radiation attenuation for the used transmission lines are shown in Chapter 5. Chapter 6 summarizes the results.

2 MR-Linac background

2.1 Basics of the magnetic resonance imaging

Magnetic resonance imaging is a medical imaging technique. It can be used both in the diagnosis and as a part of treatment of different diseases such as cancer. As a treatment tool it is used for monitoring and guiding, for example, in treatments such as MR-guided high-intensity focused ultrasound [4]. This section provides a brief background about the MRI that is relevant to the topic of this thesis.

To be able to take MRI images the patient must be positioned within a strong static magnetic field (B_0). Then a strong radio frequency (RF) pulse is applied to the patient. The RF pulse causes the body to emit another RF signal called nuclear magnetic resonance (NMR) signal. This is visualized in Figure 2. The NMR signal is received with a receive coil and sent to a computer, where an image is constructed of the received data. [5]

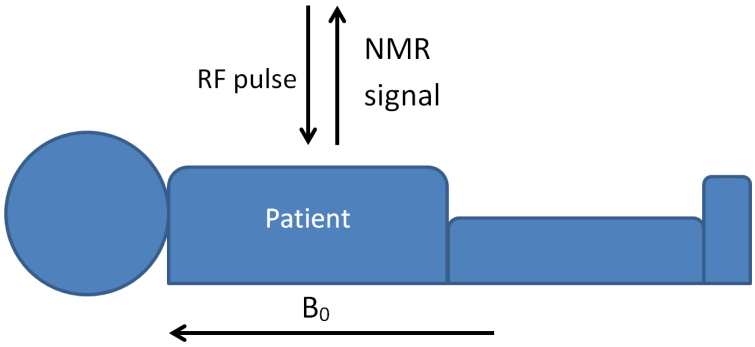

Figure 2: In MRI a radio frequency pulse is transmitted into the patient and another signal is received from the body.

When a sample containing protons is placed to a static magnetic field, the protons begin to precess about the magnetic field. The protons precess around the external magnetic field at a certain frequency. This is called the Larmor frequency and it is given as

$$f_0 = \frac{\gamma}{2\pi} B_0 \tag{1}$$

where γ is gyromagnetic ratio and B_0 is the strength of the external magnetic field [5]. For hydrogen nuclei $\gamma = 267.522 \cdot 10^6$ 1/Ts [6], so when $B_0 = 1.5$ T, the Larmor frequency is $f_0 \approx 63.87$ MHz.

Initially the protons precessing about the B_0 are out of phase and hence have no net component. When a strong (on the order of 10^3 watts) RF pulse at the Larmor frequency is applied to the protons, they begin precessing in phase with each other. When the RF pulse ceases, the protons emit their excess energy and return to their initial state. The emitted signal is the NMR signal. The magnitude of the signal is on the order of 10^{-12} watts and it decays exponentially.

2.2 Signal-to-noise ratio in MRI

Signal-to-noise ratio (SNR) is one of the key features of an MRI device. SNR is a measure that compares the signal intensity to the image and the noise level [3]. One way to define SNR is

$$\text{SNR} = \frac{signal}{noise} \tag{2}$$

where *signal* is the average brightness of pixels inside the imaged object (relative to the strength of the NMR-signal) and *noise* is the standard deviation of the pixels outside the object [3]. This is illustrated in Figure 3. Note that this definition of SNR differs from the definitions more commonly used in radio engineering.

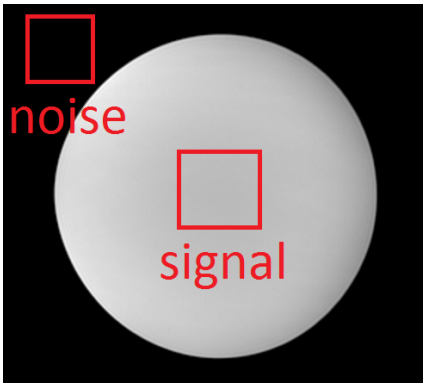

Figure 3: Signal-to-noise ratio in MRI is the ratio of the signal and noise level.

2.3 Receive coils

The receive (Rx) coil is a sensitive antenna tuned to the Larmor frequency. The oscillating magnetic field of the NMR signal induces a small current to the receive coil. This analog signal is then amplified in a low-noise preamplifier of the Rx coil and sent to an analog-to-digital converter. Traditional MRI receive coils are positioned as close to the imaging volume as possible typically on top and under the lying patient. Receive coils used in radiotherapy cannot touch the patient because that might cause shaping of internal organs and tumors.

The simplest possible Rx coil consists of only one loop element. In modern MRI systems the Rx coil is usually a phased array coil as described in [2] consisting of 4-32 coil elements. Figure 4 represents a phased array coil structure with four coil elements.

Rx coils with only one loop element can have either a large imaging area or a high SNR. A bigger loop gives a bigger imaging area and a smaller loop gives a higher SNR. However, with phased array coils it is possible to achieve images from large area while maintaining a high signal-to-noise ratio. The trade-offs of smaller loops are increased data processing requirements and reduced imaging depth. A rule of thumb in receive coil design is that the highest possible SNR of a circular coil loop is achieved from distance that equals the diameter of a circular loop. [2]

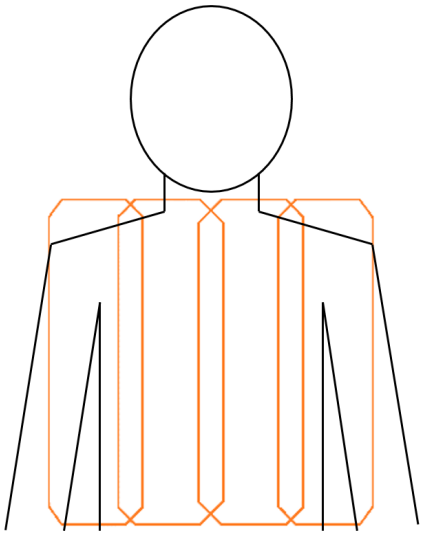

Figure 4: A receive coil with four loop elements on top of a patient. Neighbouring loops are overlapped to eliminate interactions with each others.

One design challenge with phased array coils is to isolate the separate loop elements to prevent coupling [3]. Coupling introduces unwanted signals to loop elements which increases *noise* in Equation (2) and causes a drop in SNR.

Coupling of the neighbouring elements can be diminished by geometrically overlapping the adjacent loops [2] as in Figure 4. Note that the overlapping decouples only the neighbouring loop elements. In a phased array coil such as in Figure 4 there would still be some coupling between, e.g., the first and the third elements. However, the coupling from non-neighbouring loops is relatively small (coupling coefficient is in the range of 1 %).

Each loop element of a receive coil has a preamplifier that amplifies the weak current induced by the NMR signal. This amplified analog signal is transmitted to the digitization unit through a transmission line. As with the loop elements the coupling from transmission lines to loops or other transmission lines should be minimized to prevent a decrease in the SNR. Traditionally coaxial cables are used because of their good isolation to the surrounding environment.

2.4 Linear accelerator

The linear accelerator is a device used in radiation treatments for patients with cancer. It generates high energy X-rays used to destroy cancer cells. The radiation is generated by accelerating electrons in a waveguide and colliding the accelerated electrons to a heavy metal target. The collision produces high energy photons in the Bremsstrahlung process.

These photons are directed to the patient's tumor and shaped to conform the shape of the tumor. In the MR-Linac of this thesis work the maximum field size at the center of the system is a 22 cm $\times$ 57 cm rectangle.

The photon spectrum depends on the energy of the accelerated electrons. The

spectrum is continuous from almost zero to the maximum energy of initial electrons with the peak around 1/3 of the maximum energy. In the Linac related to this thesis work the electrons have a energy of about 7 MeV. This means that the median photon has a energy of about 2 MeV. This energy is used in the later Linac radiation attenuation calculations.

2.5 MR-Linac

Two big drawbacks in radiotherapy are the effects of the Linac radiation on healthy tissue [7] and the uncertainties about the location and shape of the tumor [1]. These limitations restrict the maximum radiation dose of the treatment. This problem can be solved using image guided radiotherapy with MRI. A successful integration of a linear accelerator and a 1.5 T MRI device is reported in [1]. The term MR-Linac is used for the integration of these two systems.

When designing receive coils for MR-Linac there are two important design criterias that must be met. First the coil should attenuate the Linac radiation as little as possible. The attenuation should be as uniform as possible because the radiation can be applied from all directions of the transverse plane of the patient. Secondly the coil and especially the electronic components of the coil should withstand the effects of the Linac radiation. Both of these topics are discussed in more detail in Section 2.7 and Section 2.8.

The area of the Rx coil where the Linac radiation passes through is called the radiation window. Visualization of a radiation window on a receive coil is shown in Figure 5. The size of the radiation window is determined by the maximum rectangular Linac field size used. In MR-Linac system related to this thesis the maximum beam size is 22 cm in the head-feet direction. This sets the bare minimum of the radiation window length but in practice it must be longer. A radiation window length of 30 cm is used in this thesis work. In the left-right direction the radiation window must reach the whole width of the coil because the radiation can be applied from all directions of the patients transverse plane.

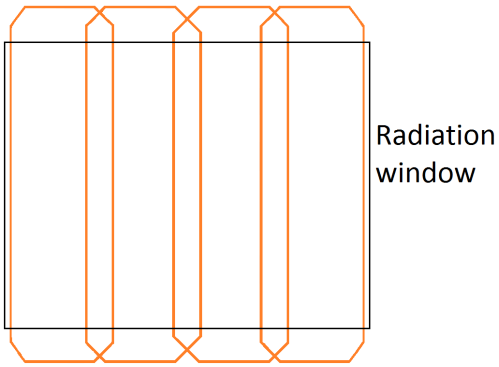

Figure 5: Radiation window in a phased array coil with four coil elements.

To achieve minimal Linac radiation attenuation the radiation window area of the receive coils should be as thin as mechanically possible and/or made of low-density

materials. Also, the electronic components, such as preamplifiers, should be moved outside the radiation window.

If a very high SNR is required from a MR-Linac receive coil, it can be achieved with smaller loops. One possible loop geometry with smaller loops is presented in Figure 6. With this kind of loop geometry the received NMR signal must be transmitted through the radiation window. Traditional coaxial cables cannot be used because of two reasons: the amount of metal in the relatively big cable attenuates Linac radiation and the round shape of the cable disperses the radiation. This thesis work focuses to study alternative transmission line methods for Linac compatible receive coils.

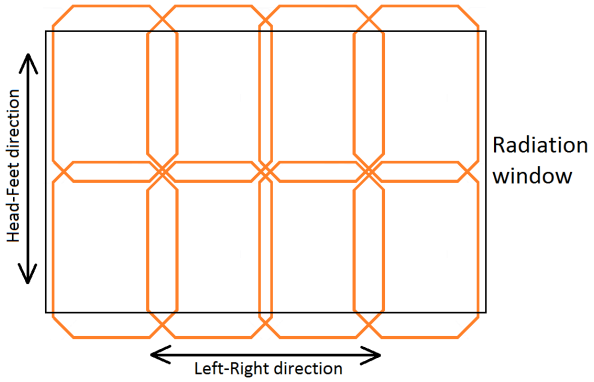

Figure 6: Phased array coil with coil elements both in the left-right and in the head-feet direction.

2.6 Sensitivity encoding

Sensitivity encoding (SENSE) is a faster way of acquiring MR images with a phased array coil. It applies the knowledge of the sensitivities of each coil elements. The acquisition time can be reduced by a factor between one and the number of coil elements. Note that the factor does not have to be an integer. More detailed description about SENSE can be found in [3].

With a coil such as in Figure 5 where all coil elements are in horizontal (left-right) direction SENSE can be used only in horizontal direction. If images are taken in head-feet direction we need to have two or more rows of coil elements in that direction. With a loop geometry such as in Figure 6 SENSE could be used in head-feet directio reducing the acquisition time by a maximum factor of two.

When using SENSE in head-feet direction with Linac compatible MRI device the amplified NMR signal must be transmitted through the radiation window. The possibilities to have higher SNR and to be able to use SENSE in head-feet direction are the motivators for this thesis work. The MRI and Linac compabilities set certain requirements for the used transmission line technologies which are discussed in the coming sections.

2.7 Radiation resistance

The ionizing high-energy radiation of a linear accelerator can cause degradation of mechanical and electrical properties of materials in MR-Linac components. The higher the radiation resistance of a component the longer the expected lifetime of the component. The estimated 10 years total dose for MR-Linac receive coils is 240 kGy.

The possible degeneration of the used materials due to the cumulative lifetime radiation dose can lead to malfunctioning of the system and to safety problems. Used materials must be selected carefully to achieve a good reliability to the system. Term radiation resistance is used to describe materials ability to withstand ionizing radiation.

If a material in MR-Linac component is suspected not to withstand its lifetime radiation dose there are four alternative workarounds:

1. The lifetime of the component can be shortened. In practice this means that the component should be changed at regular intervals.

2. The component can be relocated to a position where it is exposed to less radiation.

3. The component can be shielded, e.g., with wolfram plates. However, shielding with heavy metals is impractical in many cases because it can increase the weight of the component considerably.

4. The material can be changed to a more radiation resistive one.

For transmission lines passing through the radiation window in MR-Linac receive coils the relocation or shielding are not possibilities. By choosing an insulator material with a good radiation resistance the transmission lines can be designed to withstand the effects of Linac radiation. Polyimide, for example, is a polymer that is widely used in demanding environments and has excellent radiation resistance. It is known to withstand a total dose of 10 MGy [8].

2.8 Linac radiation attenuation

Before the Linac radiation reaches the patient it must travel through the MRI system of the MR-Linac. All system parts located in the radiation window between the linear accelerator and the patient cause attenuation to the radiation. This attenuation should be minimized when designing MR-Linac components. Also the attenuation should be as uniform as possible at the radiation window to ensure an even distribution of radiation to the tumor.

Relative intensity of a X-ray beam penetrating a material with mass thickness x and density ρ, can be calculated as

$$\frac{I}{I_0} = e^{-\frac{\mu}{\rho}x} \tag{3}$$

where μ/ρ is the mass attenuation coefficient and x is the mass thickness which is obtained by multiplying the thickness t with the density of the material ρ, i.e., $x = \rho t$ [9]. From the equation above we can define the attenuation α in percentage as

$$\alpha = (1 - e^{-\frac{\mu}{\rho}\rho t}) \cdot 100\%. \tag{4}$$

Mass attenuation coefficient of a material is dependent of the energy of the radiation. Measured μ/ρ values for different elements and compounds are listed for example in [9]. For mixtures and compounds mass attenuation coefficients can be calculated as

$$\mu/\rho = \sum_i w_i(\mu/\rho)_i \tag{5}$$

where w_i is the fraction by weight of the i^{th} atomic constituent [9].

An accurate estimate for the fraction by weight can be calculated by dividing the sum of protons and neutrons in a atom with a sum of all the protons and neutrons in the molecule. This approximations does not take into account the mass of the electrons since it is insignificantly small compared to the mass of protons and neutrons.

3 Transmission lines

In this chapter four different transmission lines are introduced: coaxial cable, micro-coaxial cable, microstrip line and coplanar waveguide. Also the requirements for a transmission line passing through the radiation window in MR-Linac are given and the topic of manufacturing of the transmission lines to a printed circuit board is discussed.

3.1 Coaxial cable

Coaxial cable is a widely used transmission line that consists of an inner conductor surrounded by an insulating dielectric which is surrounded by an outer conductor. The structure of a coaxial cable is shown in Figure 7.

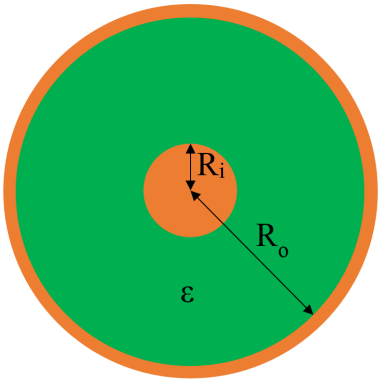

Figure 7: Cross-section of a coaxial cable.

Due to its structure the coaxial cable has a very good isolation; the outer conductor shields the cable from surrounding interferences. Conversely, the transmitted signal leaks very little outside the outer conductor.

The characteristic impedance of a coaxial cable can be calculated as

$$Z_0 = \frac{\sqrt{\varepsilon/\mu}}{2\pi} \ln(\mathrm{R_o}/\mathrm{R_i}), \tag{6}$$

where ε is the permittivity of the insulator, μ is the permeability of the insulator, $\mathrm{R_o}$ is the radius of the outer conductor and $\mathrm{R_i}$ is the radius of the inner conductor [10].

Coaxial cables' capability to carry weak signals that cannot tolerate interference from the outside environment make them desirable choice as a transmission line used in MRI receive coils. However, in MR-Linac the relatively large and round shape of traditional coaxial cables attenuates and disperses the Linac radiation significantly and un-evenly. This leads to unpredictable radiation dose delivery which makes traditional coaxial cables unusable alternative to transmit the received signal through the radiation window in MR-Linac receive coils.

3.2 Micro-coaxial cable

Micro-coaxial (MCX) cables are coaxial cables with remarkably small diameters. They are commercially available from total diameter starting from 0.15 mm. The extremely small diameter makes MCX a potential alternative for transmission lines used in MR-Linac because they cause little attenuation to the Linac radiation.

As a drawback the MCXs are expected to have more resistive losses compared to traditional coaxial cables due to smaller dimensions. Another concern about the micro-coaxials is the insulator materials ability to withstand the linear accelerator's radiation. At the time of writing this commercial MCX cables are available only with PFA (perfluoroalkoxy) or FEP (fluorinated ethylene propylene) as the insulation material.

PFA and FEP are known to have similar properties with Teflon (polytetrafluoroethylene). Teflon powders after a dose of 100 kGy [8]. Some insulation materials such as PEEK (polyetheretherketone) are marginally affected by radiation doses > 10 MGy [11].

The poor radiation resistance properties of perfluoroalkoxy make PFA and FEP insulated micro-coaxial cables unappealing alternatives for transmitting the RF-signal through the radiation window in MR-Linac. However, due the unavailability of radiation resistive MCXs at the moment, a PFA filled micro-coaxial cable is used in this thesis work to provide usability information about MCX's RF properties. Used cable was Temp-Flex 50MCX-37 whose total diameter was 0.3 mm.

3.3 Microstrip line

Microstrip line is a popular transmission line that is easy to manufacture on a PCB. The geometry of a microstrip line is shown in Figure 8. Mictrostrip consists of three components: conductor (on top), dielectric substrate (in the middle) and ground plane (at the bottom).

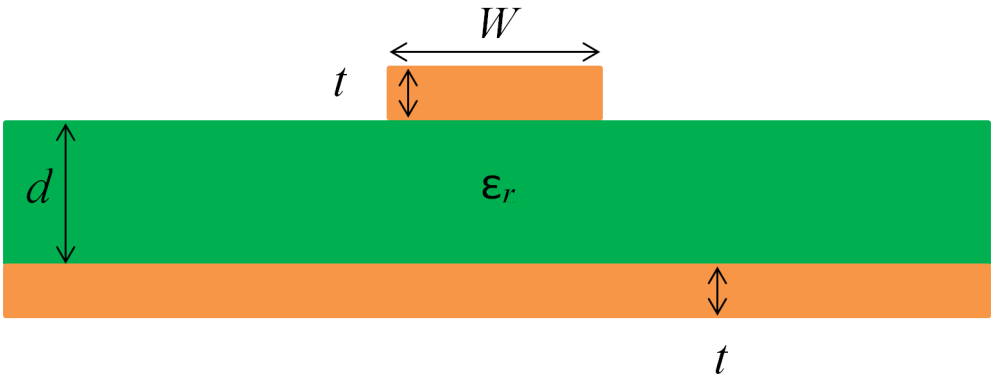

Figure 8: Cross-section of a microstrip transmission line.

When designing a microstrip line first we must determine the effective dielectric

constant ε_l. Its approximate value is

$$\varepsilon_l = \frac{\varepsilon_r + 1}{2} + \frac{\varepsilon_r - 1}{2} \frac{1}{\sqrt{1 + 12d/W}} \tag{7}$$

where d is the thickness of the dielectric and W is the width of the conductor [12]. When we know the ε_l we can solve Z_0. For cases $W/d \geq 1$ the characteristic impedance can be calculated as [12]

$$Z_0 = \frac{120\pi}{\sqrt{\varepsilon_l}[W/d + 1.393 + 0.667 \ln(W/d + 1.444)]}. \tag{8}$$

3.4 Coplanar waveguide

Coplanar waveguide (CPW) is a planar transmission line. Compared to the microstrip line, CPW has a conducting metal only in one layer on top of the dielectric substrate as shown in Figure 9. The transmission line consists of dielectric substrate at the bottom, center conductor on top and ground planes at the both sides of the conductor.

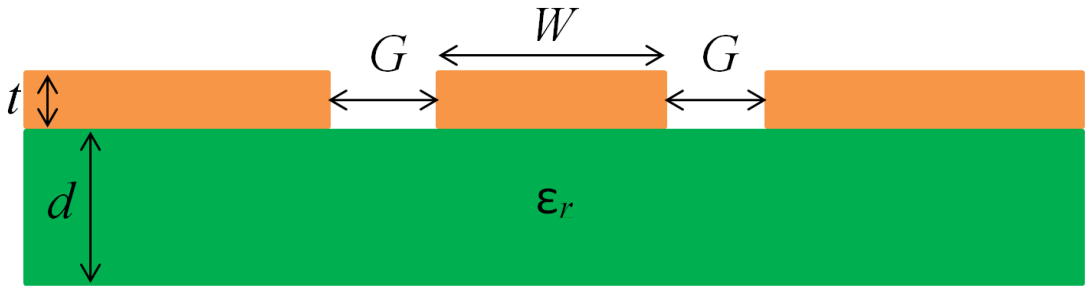

Figure 9: Cross-section of a coplanar waveguide.

3.5 MR-Linac environment requirements for transmission lines

To be both MRI and Linac compatible there are several requirements for the used transmission line method:

1. The transmission line should attenuate the linac radiation as little as possible. In practice this means minimizing the structure and especially the conductor thickness
2. The transmission line should work at the Larmor frequency of the MRI system
3. Coupling between the coil loops and the transmission lines should be minimized
4. Coupling between transmission lines should be minimized
5. Used materials must be non-magnetic
6. Used materials should withstand the high energy X-ray radiation without decrease in functionality.

3.6 Printed circuit boards

In modern Rx coils the coil loops are manufactured on a printed circuit board (PCB). Figure 10 shows an example of PCB receive coil loops. Because the loops are on a PCB, it would be practical to implement also the transmission lines to the same PCB. From the previously introduced transmission lines microstrip line and CPW are manufacturable on a PCB.

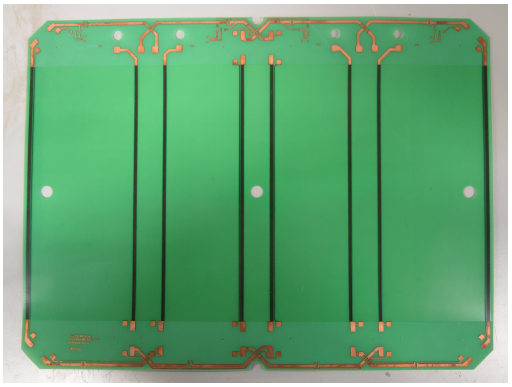

Figure 10: Four receive coil loops manufactured on a printed circuit board. The gaps in the loops are reserved for preamplifiers and tuning electronics.

4 Measurements

4.1 First prototypes

The purpose of the first prototypes was to get an initial feeling of the feasibility and the manufacturability of the microstrip line and coplanar waveguide. The biggest interest was to study changes in S_{11} and transmission coefficient (S_{21}). Three prototype transmission lines are shown in Figure 11.

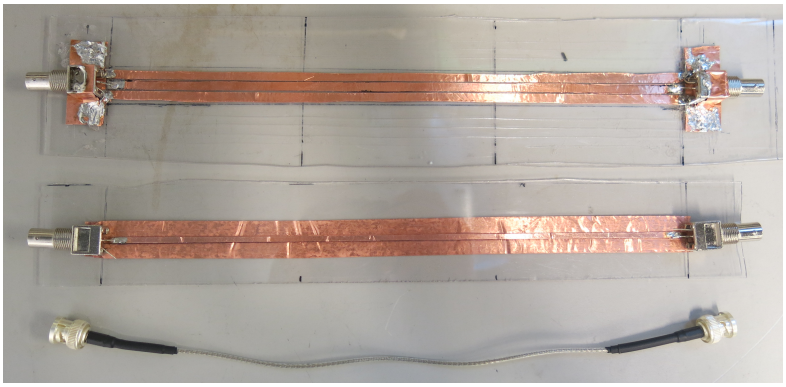

Figure 11: Three prototype transmission lines. From bottom to top: coaxial cable (used as a reference), microstrip line and coplanar waveguide.

4.1.1 Reference coaxial cable

In traditional Rx coils coaxial cables are used to transfer the received signal. A 50 Ω coaxial cable was built to test the measurement setup and to get reference results for the prototype transmission lines. The length of the coaxial cable was 30 cm and its total diameter was 2.8 mm (RG174). The used cable type was chosen as a reference because it is used in other Philips MRI receive coils.

4.1.2 Microstrip prototype

The microstrip prototypes were built with copper tape on 1 mm thick polycarbonate plastic, whose relative permittivity was estimated to be $\varepsilon_r = 2.9$. Thickness of the copper tape was 50 μm.

In the prototype there were two changeable design parameters: the width of the top conductor (W) and the width of the ground plane (W_{GND}). With Equations (7) and (8) it can be calculated that impedance $Z_0 = 50\ \Omega$ is achieved when the width of the conductor is $W \approx 3$ mm.

For the second parameter, W_{GND}, there was no design equation. Three different ground widths (19 mm, 12 mm and 8 mm) were tested and effects for S_{11}, S_{21} and coupling were recorded. Results are summarized in Section 4.1.4.

4.1.3 Coplanar waveguide prototype

The CPW prototypes were built with copper tape on 2 mm thick polycarbonate plastic, whose relative permittivity was estimated to be $\varepsilon_r = 2.9$. Thickness of the copper tape was 50 μm.

Coplanar waveguide has three design parameters: width of the center conductor (W), width of the gap between the conductor strip and the ground strips (G), and the width of the ground planes (W_{GND}).

In CPW the impedance is determined by the ratio of W and G. This means that it is possible to reduce the size of a CPW without a limit. However smaller size increases the resistive losses. Because the first prototypes were handmade, it was difficult to manufacture very small dimensions. Two different gap widths were tested: $G = 1$ mm and $G = 0.5$ mm.

When the gap widths were chosen the width of the center conductor was calculated with AWR Design Environment. When $G = 1$ mm, $Z_0 = 50\ \Omega$ is achieved with $W = 36$ mm. The width of 36 mm was considered to be impractically large and it was noticed that using a clearly smaller width $W = 19$ mm gives a characteristic impedance of $Z_0 = 56\ \Omega$. This was considered to be "close enough" and was used for practical reasons. When the $G = 0.5$ mm, a center conductor width of 5 mm was used. With these widths the $Z_0 = 60\ \Omega$.

As with the microstrip line design, there was no equation for the W_{GND}. Two different ground widths were tested: 5 mm and 19 mm.

4.1.4 Measurement results

The measurements were done using a network analyzer whose ports 1 and 2 were connected to the transmission line's ends. Measured S_{11} and S_{21} are presented in Table 1.

Table 1: S_{11} and S_{21} of the built transmission lines at 63.87 MHz. All tranmission line dimensions are in mm.

	S_{11} (dB)	S_{21} (dB)
Reference coaxial cable	-35	-0.1
Microstrip, $W = 3$, $W_{GND} = 19$	-21	-0.1
Microstrip, $W = 3$, $W_{GND} = 12$	-20	-0.1
Microstrip, $W = 3$, $W_{GND} = 8$	-20	-0.1
CPW, $W = 19$, $G = 1$, $W_{GND} = 19$	-17	-0.1
CPW, $W = 19$, $G = 1$, $W_{GND} = 5$	-15	-0.2
CPW, $W = 5$, $G = 0.5$, $W_{GND} = 19$	-16	-0.2
CPW, $W = 5$, $G = 0.5$, $W_{GND} = 5$	-15	-0.2

Following observations were made from the measurements:

- S_{11} values of the microstrip lines are $\leqslant$ -20 dB. S_{11} values of the coplanar waveguides are in the range of -17...-15 dB. These values are expected to get better when industrially manufacturing the transmission lines to PCB.
- S_{21} values for the microstrip and CPW are -0.1...-0.2 dB. This tells that there are no significant losses in the transmission lines.
- Reducing the W_{GND} of microstrip line does not have a dramatic effect on S_{11} nor S_{21}.
- Reducing the W_{GND} of a CPW slightly increases the S_{11}. However, $W_{GND} = W$ seems to give still reasonable results ($S_{11} \leqslant$ -15 dB).

4.2 PCB transmission lines

After building and testing the first prototype transmission lines various microstrip lines and coplanar waveguides were designed on printed circuit boards. First step of the design was to choose the dielectric thickness and material.

To fulfill the radiation withstanding requirement DuPont polyimide (PI) is chosen as PCB dielectric material. It is used in high-reliability applications and can resist a long-term harsh environments. Polyimide can withstand high-energy radiation up to 10 MGy doses with little or no changes in either its physical or electrical properties [8]. The dielectric is commercially available in thicknesses from 25.4 μm to 152.4 μm. Thinner dielectric causes less Linac radiation attenuation but it also causes difficulties in transmission line design. The thickness was chosen to be 101.6 μm.

Conductor material was chosen to be copper because of its excellent conductivity. A study in [13] shows that a receive coil can be made more radiation transparent by using aluminum as a conductor instead of copper. However, the lower conductivity of the aluminum causes additional losses and lowers SNR which is undesirable so copper is used instead.

The design of the PCB transmission lines was done with the following specifications:

- Used dielectric is DuPont polyimide (Product code: AP8545R, $\varepsilon_r = 3.4$ and thickness $d = 101.6$ μm)
- Used conductor is copper (thickness $t = 18$ μm and coductivity $\sigma = 5.8 \cdot 10^7$ S/m)
- $f_0 = 63.87$ MHz (Larmor frequency of a 1.5 T MRI system)
- $Z_0 = 50$ Ω
- Length of the transmission line = 35 cm
- Minimum conductor width = 0.1 mm (Manufacturer limit)
- Minimum condutor spacing = 0.1 mm (Manufacturer limit)

The design was done using AWR Design Environment. Some of the designed transmission lines are shown in Figure 12.

Figure 12: Transmission lines from top to bottom: micro-coaxial cable, microstrip line, coplanar waveguide and multiconductor microstrip line with two top conductors on a common ground plane.

4.2.1 Microstrip lines on PCB

With chosen conductor and dielectric properties and W = 0.3 mm the theoretical S_{11} = -33 dB and the S_{22} = -0.2 dB. Four different ground widths were tested: 6 mm, 4 mm, 2 mm and 1 mm. Designed microstrip lines and their measured S_{11} and S_{21} values are summarized in Table 2.

Table 2: Measured S_{11} and S_{21} values of the designed microstrip lines.

W (mm)	W_{GND} (mm)	S_{11} (dB)	S_{21} (dB)
0.3	6	-19	-0.4
0.3	4	-19	-0.4
0.3	2	-20	-0.4
0.3	1	-21	-0.3

4.2.2 Coplanar waveguides on PCB

When desinging the CPWs it was assumed that making the gap in CPW structure smaller limits the surrounging electromagnetic fields to a smaller area thus reducing the coupling to receive coil loops. From the first prototype measurements it was also noticed that the W_{GND} should be the same order of magnitude with the W.

With the smallest manufacturable gap (G = 0.1 mm) three different center conductor widths were tested: 0.5 mm, 1.0 mm and 1.8 mm. Various ground widths were tested with these center conductor widths. Also 0.2 mm gap was tested with W = 1.8 mm and W_{GND} = 1.9 mm. Designed CPWs with their measured S_{11} and S_{21} values are represented in Table 3.

Table 3: Summary of the designed coplanar waveguides and their measured S_{11} and S_{21} values.

G (mm)	W (mm)	W_{GND} (mm)	W_{total} (mm)	S_{11} (dB)	S_{21} (dB)
0.1	1.8	2	6	-37	-0.2
0.1	1.8	1	4	-32	-0.2
0.1	1	2	5.2	-24	-0.3
0.1	1	1	3.2	-23	-0.3
0.1	0.5	1	2.7	-17	-0.4
0.1	0.5	0.5	1.7	-16	-0.4
0.2	1.8	1.9	6	-16	-0.3

4.3 Coupling measurement

The coupling from a transmission line to a receive coil loop heavily depends on the position of the transmission line. A coupling measurement was carried out where the transmission lines were positioned along a head-feet direction on a phased array coil with four loops and fed with a 64 MHz signal. The tested transmission lines were moved across the receive coil in the left-right direction and the coupled voltage to the Rx coil loops was measured with an oscilloscope. Each loop had a 28 dB preamplifier.

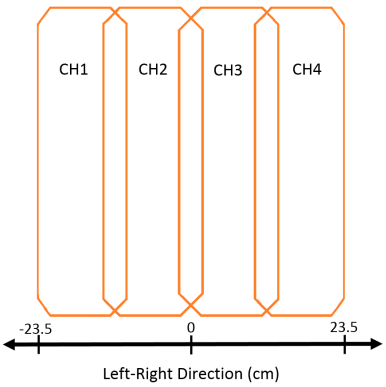

Figure 13: Geometry of the receive coil used in the coupling measurements. Channels are numbered from one to four from left to right. Position 0 cm stands for the center of the coil, position -23.5 cm the outer side of channel 1 and the position 23.5 cm the outer side of channel 4. Tested cables were aligned in the head-feet direction.

Because the receive coil is such a sensitive antenna all external noise sources must be minimized to successfully measure the coupling from a nearby transmission line. First a network analyzer measurement was tried but the coupling from the measurement cables could not be eliminated. To be sure that the measured voltage is coupled only from the transmission line there can be no other cables in the test setup. A 64 MHz test source was built to feed the transmission lines in the coupling

measurements.

The test source consisted of a 64 MHz crystal oscillator which +5 V_{DC} input voltage was implemented with a 5 V regulator that was fed with 9 V alkaline battery. Also a first degree LC lowpass filter was implemented at the output of the oscillator to block unwanted harmonic distortion. The test source is shown in Figure 14. All the components were encapsulated inside an aluminum box to prevent it from interfering with the coupling measurement. The signal was transmitted with a female BNC connector from the box. The output of the test source was 64 MHz sine wave with a peak-to-peak voltage of 1.85 V.

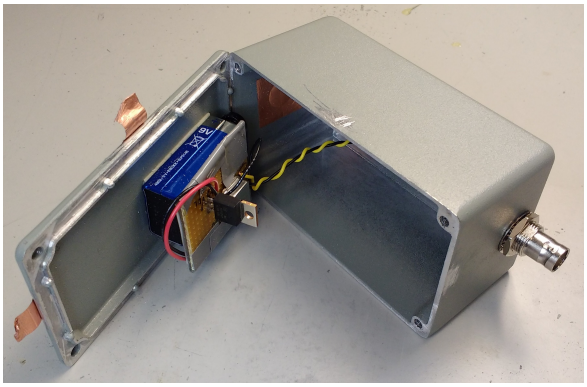

Figure 14: Opened test source. It consisted of a 9 V battery, 5 V regulator, 64 MHz crystal oscillator and a LC lowpass filter enclosed inside a metal box.

The test source was used to feed the sine wave through the tested cable that was terminated with a 50 Ω load. The coupled signal was amplified with a 28 dB preamplifier of the loop and the amplified peak-to-peak voltage was measured with an oscilloscope with 29 positions.

4.3.1 Coupling from a micro-coaxial cable

Measurement results for micro-coaxial cable are shown in Figure 15.

From the results presented in Figure 15 it can be seen that there is least coupling to a loop in the middle of the loop. Coupling is strongest on top of the loop sides when the transmission line runs along the loop. After the points of biggest coupling the coupling reduces steadily when moving away from the loop. This kind of coupling was expected because when the transmission line runs through the center of the loop there should be minimal coupling due the symmetry of the position.

In a receive coil with four loop elements in a row the optimal positions for MCXs are a bit to the edges from the middle of the outermost loops (≈ + 18.25 cm and -18.25 cm in Figure 15). There the total coupling to all loops is the least. This means that also the signal received by the middle loops should be transmitted through the center of the outermost loops. For micro-coaxial cables this is not a problem since the total diameter of the cables is only 0.3 mm.

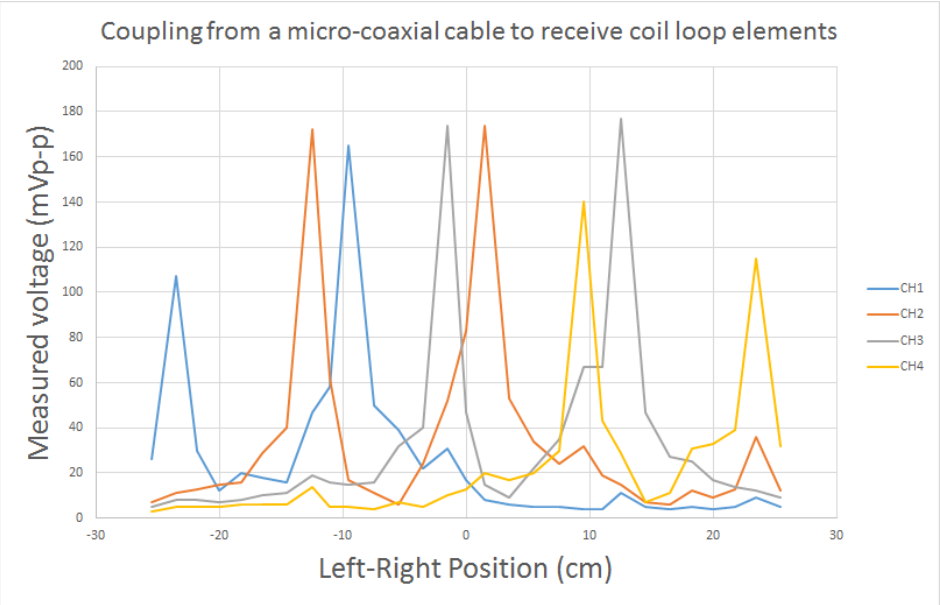

Figure 15: Measured coupling from a micro-coaxial cable to four loop elements of a receive coil.

4.3.2 Coupling from a microstrip line

Coupling measurement was done to all four microstrip lines. Smallest coupling was achieved with the microstrip line with the biggest ground plane ($W_{GND} = 6$ mm). Measurement results for the microstrip line with the 6 mm ground plane are shown in Figure 16.

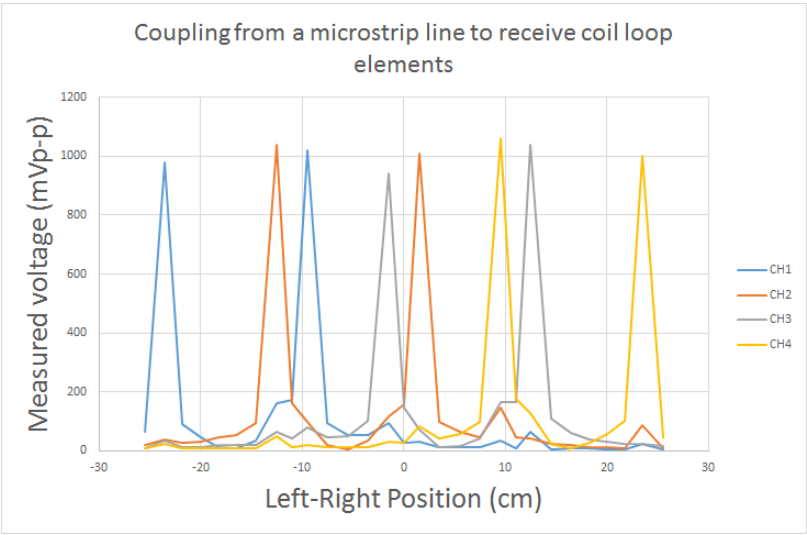

Figure 16: Measured coupling from a microstrip line ($W = 0.3$ mm and $W_{GND} = 6$ mm) to four loop elements of a receive coil.

The coupling from the microstrip line shows a similar trend as the coupling from

the micro-coaxial cable. However, in every position the coupling is clearly stronger especially on top of the conductors. In the middle of the loops the coupling is in the same order of magnitude as the coupling from the micro-coaxial cable.

As with the MCX the optimal positions for the transmission lines are in +18.25 cm and -18.25 cm. The received signals from loops 1 and 2 should be transmitted through loop 1 and the signals from loops 3 and 4 should be transmitted through loop 4.

To simplify the transmission of two signals with two adjacent microstrip lines a multiconductor microstrip line was designed with two top conductors. It consisted of two 0.3 mm top conductors separated 6 mm away from each other on a 12 mm ground plane. It was designed on the same substrate as the other PCB transmission lines (DuPont Pyralux AP8545R) and was 35 cm long.

4.3.3 Coupling from a coplanar waveguide

Coupling measurement was done to all seven coplanar waveguides. Smallest coupling was achieved with the CPW with the $W_{GND} = 2$ mm, $W = 1$ mm and $G = 0.1$ mm. Measurement results for the CPW with the least coupling are shown in Figure 17.

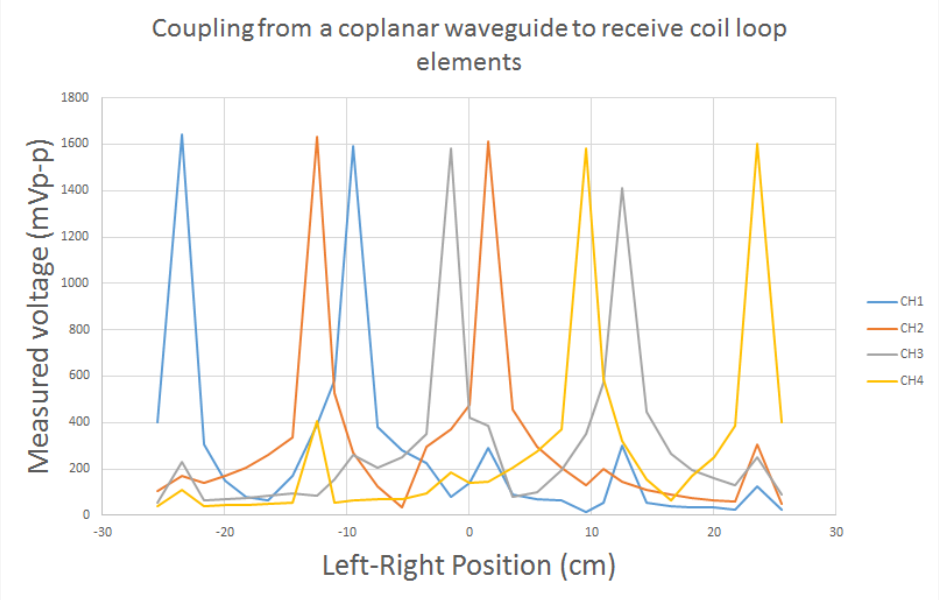

Figure 17: Measured coupling from a coplanar waveguide ($W = 0.1$ mm, $W_{GND} = 2$ mm and $G = 0.1$ mm) to four loop elements of a receive coil.

CPW had clearly strongest coupling compared to the micro-coaxial cable and the microstrip line. Even in the positions where the total coupling was least there was more coupling than with the MCX's worst positions.

4.4 Signal-to-noise ratio measurements

To compare the available image quality with the chosen transmission lines a SNR measurement was carried out. The measurement was done using a 1.5T MR-Linac prototype system.

A receive coil with four loop channels was placed on top of a 400 mm diameter phantom. The phantom is filled with liquid that is visible in MR images. The phantom and the Rx coil were positioned in the radiation window of the MR-Linac system. The measurement setup is shown in Figure 18. An MR image of the phantom was taken and the signal-to-noise ratio of the image was determined as described in Section 2.2.

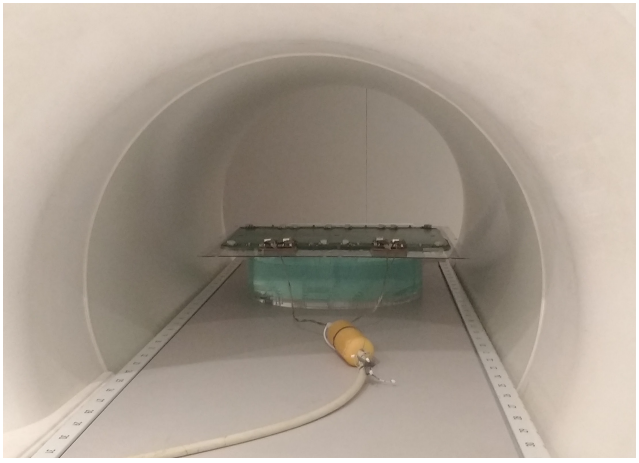

Figure 18: The SNR measurement setup: The receive coil on top of the 400 mm phantom in the radiation window of the MR-Linac system.

To be able to evaluate the quality of the acquired images with the tested transmission lines a reference SNR measurement was done. In the reference measurement MR image was acquired without additional transmission lines, i.e., no signal was transmitted through the radiation window. SNR of the reference measurement was 186.

When taking MR images with the tested transmission lines the receive coil was flipped 180 degrees to place the preamplifiers to the opposite side of the receive coil. This way the signal could be transmitted through the radiation window. The reference measurement setup and the setup with the micro-coaxial cables are shown in Figure 19.

The micro-coaxial cables from channels 1 and 2 were twisted together and placed to position -18.25 cm in the left-right direction. Similarly the MCXs from channels 3 and 4 were twisted and placed to position +18.25 cm. Twisting the cables together reduces coupling between the cables. In positions -18.25 cm and +18.25 cm the total coupling to the receive coil loops was least as described in Sections 4.3. SNR of the image when using the micro-coaxial cables was 128.

The multiconductor microstrip lines described in Section 4.3.2 were also positioned to -18.25 cm and +18.25 cm in the left-right-direction. SNR of the image with

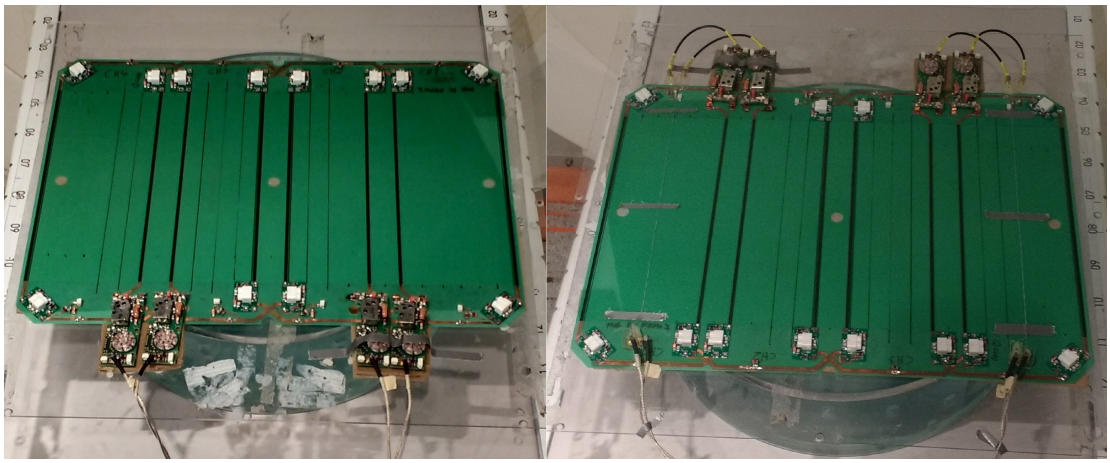

Figure 19: Left: Reference measurement setup. Right: Measurement setup with the twisted MCXs. The preamplifiers were on the opposite side of the Rx coil to be able to transmit the signal through the radiation window.

microstrip lines was 176.

When using the coplanar waveguide only noise was visible in the MR images. The coupling to the receive coil loops from the CPW was so strong (see Section 4.3.3) that it was determined to be unusable for transmitting the received signal through the radiation window.

The measured signal-to-noise ratios values and calculated relative SNRs are presented in Table 4.

Table 4: Measured signal-to-noise ratios. Relative SNR values are calculated by dividing the measured SNR values with the reference measurement SNR.

	SNR	Relative SNR
Reference measurement	186	100 %
Micro-coaxial cable	128	69 %
Microstrip line	176	95 %
Coplanar waveguide	N/A	N/A

Microstrip line gives clearly the highest SNR compared to micro-coaxial cable and coplanar waveguide. An MR image using microstrip lines to transmit through the radiation window is shown in Figure 20.

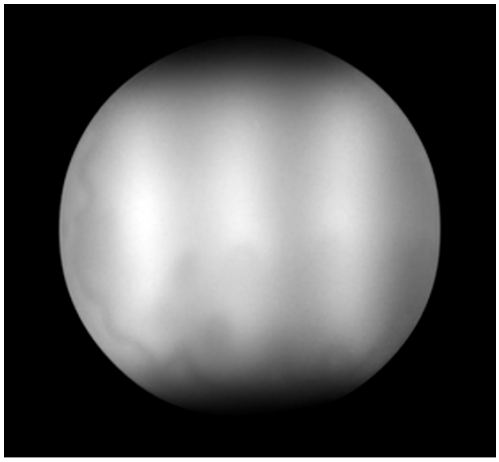

Figure 20: An MR image acquired with the multiconductor microstrip line.

5 Radiation attenuation calculations

A minimal Linac radiation attenuation is required for transmission lines running through the radiation window of MR-Linac. The percentage attenuation of a transmission line can be calculated with Equation (4). If the material is a mixture or a compound, the mass absorption coefficient must be calculated with Equation (5) before determining the attenuation. Calculations in this chapter are done to photons with 2 MeV energy.

5.1 Attenuation due to micro-coaxial cable

The micro-coaxial cable has four cylindrical layers:

- Center conductor. 75 μm thick copper.
- Insulator. 63 μm thick PFA.
- Outer conductor. 31 μm thick copper.
- Jacket. 25 μm thick PFA.

For copper $\rho_{\mathrm{Cu}} = 8.96$ g/cm^3 and $\mu/\rho_{\mathrm{Cu}} = 4.205 \cdot 10^{-2}$ cm^2/g at 2 MeV. Using Equation (4) the attenuation of the 31 μm outer copper layer can be calculated as

$$\alpha = (1 - e^{-\frac{\mu}{\rho}_{\mathrm{Cu}} \rho_{\mathrm{Cu}} t}) \cdot 100\%$$

$$\alpha = (1 - e^{-4.205 \cdot 10^{-2} \frac{\mathrm{cm}^2}{\mathrm{g}} \cdot 8.96 \frac{\mathrm{g}}{\mathrm{cm}^3} \cdot 31 \cdot 10^{-4} \mathrm{cm}}) \cdot 100\% \approx 0.117\%$$

and the attenuation of the 75 μm center conductor as

$$\alpha = (1 - e^{-4.205 \cdot 10^{-2} \frac{\mathrm{cm}^2}{\mathrm{g}} \cdot 8.96 \frac{\mathrm{g}}{\mathrm{cm}^3} \cdot 75 \cdot 10^{-4} \mathrm{cm}}) \cdot 100\% \approx 0.282\%.$$

The density of PFA is $\rho_{\mathrm{PFA}} = 2.15$ g/cm^3. For PFA mass absorption coefficient Teflon values are used because of PFA's and Teflon's similarity as a material. For Teflon $\mu/\rho_{\mathrm{Teflon}} = 4.280 \cdot 10^{-2}$ cm^2/g at 2 MeV [9]. The percentage attenuation of the 25 μm PFA jacket is

$$\alpha = (1 - e^{-4.280 \cdot 10^{-2} \frac{\mathrm{cm}^2}{\mathrm{g}} \cdot 2.15 \frac{\mathrm{g}}{\mathrm{cm}^3} \cdot 25 \cdot 10^{-4} \mathrm{cm}}) \cdot 100\% \approx 0.023\%$$

and the attenuation of the 65 μm PFA insulator is

$$\alpha = (1 - e^{-4.280 \cdot 10^{-2} \frac{\mathrm{cm}^2}{\mathrm{g}} \cdot 2.15 \frac{\mathrm{g}}{\mathrm{cm}^3} \cdot 63 \cdot 10^{-4} \mathrm{cm}}) \cdot 100\% \approx 0.058\%.$$

When Linac radiation passes through the MCX it travels twice through all the other layers except the center conductor. The total percentage attenuation of a micro-coaxial cable is

$$\alpha = [1-(1-0.282/100)(1-0.058/100)^2(1-0.117/100)^2(1-0.023/100)^2] \cdot 100\% \approx 0.676\%.$$

5.2 Attenuation due to microstrip line

The designed microstrip lines consis of three layers. 18 μm thick copper layers on top and at the bottom and 101.6 μm thick PI substrate between the copper layers.

The density of copper is $\rho_{\mathrm{Cu}} = 8.96$ g/cm^3. At 2 MeV the $\mu/\rho_{\mathrm{Cu}} = 4.205 \cdot 10^{-2}$ cm^2/g [9]. For the 18 μm copper the attenuation at 2 MeV can be calculated as

$$\alpha = (1 - e^{-4.205 \cdot 10^{-2} \frac{\mathrm{cm}^2}{\mathrm{g}} \cdot 8.96 \frac{\mathrm{g}}{\mathrm{cm}^3} \cdot 18 \cdot 10^{-4} \mathrm{cm}}) \cdot 100\% \approx 0.068\%.$$

The density of polyimide is $\rho_{\mathrm{PI}} = 1.42$ g/cm^3. For the attenuation of the polyimide the mass absorption coefficient of the polyimide must be determined. To be able to calculate the μ/ρ for polyimide ($C_{20}H_{10}O_5N_2$) the fraction by weight, w, must be first determined for all atomic constituents. Carbon consists of six protons and six neutrons so its atomic mass is 12. Hydrogen consists of just one proton so its atomic mass is 1. Respectively the atomic mass of oxygen is 16 and the atomic mass of nitrogen is 14. In one PI molecule there are 20 carbon atoms, 10 hydrogen atoms, five oxygen atoms and two nitrogen atoms. The total atomic mass of a polyimide is a sum of all the atomic masses each multiplied by the number of atoms in one molecule $12 \cdot 20 + 1 \cdot 10 + 16 \cdot 5 + 14 \cdot 2 = 358$.

Now the fraction by weight can be calculated for each atomic constituents as the multiplication of the atomic mass and the number of atoms divided by the total atomic mass of PI. For carbon $w_{\mathrm{C}} = 12 \cdot 20/358 = 240/358$, for hydrogen $w_{\mathrm{H}} = 10/358$, for oxygen $w_{\mathrm{O}} = 80/358$ and for nitrogen $w_{\mathrm{N}} = 28/358$.

When the mass fractions by weight are known the mass absorption coefficient for polyimide can be calculated as

$$\mu/\rho_{\mathrm{PI}} = \frac{240}{358} \cdot \mu/\rho_{\mathrm{C}} + \frac{10}{358} \cdot \mu/\rho_{\mathrm{H}} + \frac{80}{358} \cdot \mu/\rho_{\mathrm{O}} + \frac{28}{358} \cdot \mu/\rho_{\mathrm{N}}. \tag{9}$$

The values for mass absorption coefficients for carbon, hydrogen, oxygen and nitrogen can be found in [9].

At 2 MeV the Equation (9) gives $\mu/\rho_{\mathrm{PI}} \approx 4.567 \cdot 10^{-2}$ cm^2/g. Now the attenuation of 101.6 μm polyimide can be calculated as

$$\alpha = (1 - e^{-4.567 \cdot 10^{-2} \frac{\mathrm{cm}^2}{\mathrm{g}} \cdot 1.42 \frac{\mathrm{g}}{\mathrm{cm}^3} \cdot 101.6 \cdot 10^{-4} \mathrm{cm}}) \cdot 100\% \approx 0.066\%.$$

When the Linac radiation passes through two 18 μm copper layers and a 101.6 μm polyimide layer the total attenuation of the microstip line is

$$\alpha = [1 - (1 - 0.068/100)^2 (1 - 0.066/100)] \cdot 100\% \approx 0.202\%.$$

If the microstrip line was implemented on the same PCB as the receive coil loops, there would be no need for additional substrate layer. In this kind of design the additional Linac radiation attenuation would be caused only by the two copper layers. Then the attenuation of the microstrip line would be

$$\alpha = [1 - (1 - 0.068/100)^2] \cdot 100\% \approx 0.136\%.$$

5.3 Attenuation due to coplanar waveguide

Compared to the microstrip line CPW has copper layer only on one side of the polyimide substrate. Using the same calculations as with the microstrip line the attenuation of the CPW can be calculated to be

$$\alpha = [1 - (1 - 0.068/100)(1 - 0.066/100)] \cdot 100\% \approx 0.134\%.$$

If the coplanar waveguide was implemented on the same PCB as the receive coil loops, there would be no need for additional substrate layer. In this kind of design the additional Linac radiation attenuation would be caused only by one copper layer. Then the attenuation of the CPW would be

$$\alpha = [1 - (1 - 0.068/100)] \cdot 100\% \approx 0.068\%.$$

6 Conclusions

Three signal transfer methods were tested and compared to transfer a 63.87 MHz RF-signal through a radiation window in MR-Linac receive coil. Tested transmission lines were a micro-coaxial cable, a microstrip line and a coplanar waveguide. The comparison results are summarized in Table 5. SNR values were obtained from MRI images where the received signal was transmitted through the radiation window with the tested transmission line. Radiation attenuation percentages are theoretical values calculated in Chapter 5. Radiation resistance analysis of the transmission lines was done based on the literature.

Table 5: Comparison of relative SNR, Linac radiation attenuation at 2 MeV and radiation resistivity of MCX, microstrip line and coplanar waveguide. Relative SNR is calculated by dividing the measured SNR value with the measured reference SNR value described in Section 4.4. The coplanar waveguide had such a strong coupling to the receive coil loops that its SNR value was impossible to determine.

	Relative SNR	Attenuation at 2 MeV	Radiation resistance
Micro-coaxial cable	69 %	0.678 %	$<$ 100 kGy
Microstrip line	95 %	0.202 %	$>$ 10 MGy
Coplanar waveguide	N/A	0.132 %	$>$ 10 MGy

Based on the numbers presented in Table 5 the microstrip line is the most usable for transmitting the received signal through the radiation window in MR-Linac. It has the highest SNR and a very good radiation resistance. Also if the microstrip line were implemented on the same PCB as the receive coil loops, it would cause only 0.136 % attenuation to the 2 MeV Linac radiation as discussed in Section 5.2.

Using the microstrip line for transmitting the received signal through the radiation window enables the design of MR-Linac receive coils with two coil rows in head-feet direction. With this kind of a loop geometry a higher SNR can be achieved and images can be acquired faster using sensitivity encoding in head-feet direction.

References

[1] B. W. Raaymakers, J. J. W. Lagendijk, J. Overweg, J. G. M. Kok, A. J. E. Raaijmakers, E. M. Kerkhof, R. W. van der Put, I. Meijsing, S. P. M. Crijns, and F. Benedosso, "Integrating a 1.5 T MRI scanner with a 6 MV accelerator: proof of concept," *Physics in Medicine and Biology*, vol. 54, no. 12, pp. 229–237, 2009.

[2] P. B. Roemer, W. A. Edelstein, C. E. Hayes, S. P. Souza, and O. M. Mueller, "The NMR phased array," *Magnetic Resonance in Medicine*, vol. 16, no. 2, pp. 192–225, 1990.

[3] D. W. McRobbie, E. A. Moore, M. J. Graves, and M. R. Prince, *MRI from Picture to Proton*. Cambridge University Press, 2007.

[4] H. S. Kim, J.-H. Baik, L. D. Pham, and M. A. Jacobs, "MR-guided high-intensity focused ultrasound treatment for symptomatic uterine leiomyomata: long-term outcomes," *Academic Radiology*, vol. 18, no. 8, pp. 970–976, 2011.

[5] R. H. Hashemi and G. B. William, *MRI: The Basics*. Williams & Wilkins, 1997.

[6] M. H. Levitt, *Spin Dynamics: Basics of Nuclear Magnetic Resonance*. Wiley, 2013.

[7] J. J. W. Lagendijk, B. W. Raaymakers, A. J. E. Raaijmakers, J. Overweg, K. J. Brown, E. M. Kerkhof, R. W. van der Put, B. Hårdemark, M. van Vulpen, and U. A. van der Heide, "MRI/linac integration," *Radiotherapy and Oncology*, vol. 86, no. 1, pp. 25–29, 2008.

[8] C. L. Hanks and D. J. Hamman, "Electrical insulating materials and capacitors," in *Radiation Effects Design Handbook*, ch. 3, NASA, 1971.

[9] J. H. Hubbell and S. M. Seltzer, "Tables of X-ray mass attenuation coefficients and mass energy-absorption coefficients 1 keV to 20 MeV for elements Z= 1 to 92 and 48 additional substances of dosimetric interest," tech. rep., National Institution of Standards and Technology, 1995.

[10] A. Räisänen and A. Lehto, *Radiotekniikan perusteet*. Otatieto, 2007.

[11] M. Tavlet and H. Van der Burgt, "Radiation resistance and other safety aspects of high-performance plastics by ERTA," tech. rep., CERN, 1994.

[12] D. M. Pozar, *Microwave Engineering*. Wiley, 2004.

[13] V. Rieke, A. Ganguly, B. L. Daniel, G. Scott, J. M. Pauly, R. Fahrig, N. J. Pelc, and K. Butts, "X-ray compatible radiofrequency coil for magnetic resonance imaging," *Magnetic Resonance in Medicine*, vol. 53, no. 6, pp. 1409–1414, 2005.